Biological Sciences: *Medical Sciences*

Assessing the Significance of Chromosomal Aberrations in Cancer: Methodology and Application to Glioma

Rameen Beroukhim[1,2,3,4,14], Gad Getz[1,14], Leia Nghiemphu[5], Jordi Barretina[1,2], Teli Hsueh[5], David Linhart[1,2], Igor Vivanco[5], Jeffrey C. Lee[1,2], Julie H. Huang[5], Sethu Alexander[1,2], Jinyan Du[1,2], Tweeny Kau[5], Roman K. Thomas[1,2,6,7], Kinjal Shah[1,2], Horacio Soto[5], Sven Perner[3,8], John Prensner[1,2], Ralph M. Debiasi[1,2], Francesca Demichelis[3], Charlie Hatton[1,2], Mark A. Rubin[1,3,4], Levi A. Garraway[1,2,3,4], Stan F. Nelson[5], Linda Liau[5], Paul Mischel[5], Tim F. Cloughesy[5], Matthew Meyerson[1,2,4], Todd A. Golub[1,2,4,9,10], Eric S. Lander[1,4,11], Ingo K. Mellinghoff[12] & William R. Sellers[1,2,3,4,13]

[1] Broad Institute of MIT and Harvard, 7 Cambridge Center, Cambridge, MA 02142, USA.
[2] Departments of Medical and Pediatric Oncology and Center for Cancer Genome Discovery, Dana-Farber Cancer Institute, 44 Binney St, Boston, MA 02115, USA.
[3] Departments of Medicine and Pathology, Brigham and Women's Hospital, 75 Francis St, Boston, MA 02115, USA.
[4] Departments of Medicine, Pathology, and Pediatrics, Harvard Medical School, Boston, MA 02115, USA.
[5] Departments of Medical Pharmacology, Neurology, Pathology, Human Genetics, and Neurosurgery, David Geffen School of Medicine at the University of California, Los Angeles, Los Angeles, CA, 90095, USA.
[6] Max-Planck Institute for Neurological Research with Klaus-Joachim Zülch Laboratories of the Max-Planck Society and the Medical Faculty of the University of Cologne, Gleueler Str 50, 50931 Cologne, Germany.
[7] Center for Integrated Oncology and Department I for Internal Medicine, University of Cologne, 50931 Cologne, Germany.
[8] Department of Pathology, University of Ulm, Ulm, Germany.
[9] Howard Hughes Medical Institute, Chevy Chase, MD 20815, USA.
[10] Department of Medicine, Children's Hospital Boston, Boston, MA 02115, USA.
[11] Whitehead Institute for Biomedical Research, 9 Cambridge Center, Cambridge, MA 02142, USA.
[12] Human Oncology and Pathogenesis Program and Department of Neurology, Memorial-Sloan-Kettering Cancer Center, 1275 York Ave, New York, NY 10021, USA.
[13] Novartis Institutes for BioMedical Research, 250 Massachusetts Ave, Cambridge, MA 02139, USA.
[14] Contributed equally.

Correspondence should be addressed to W.R.S. (ph. 617-871-7069, fax 617-871-3453; william.sellers@novartis.com) or I.K.M. (ph. 646-888-2766, fax 646-422-0856; mellingi@mskcc.org).

Running count:

Abstract

Comprehensive knowledge of the genomic alterations that underlie cancer is a critical foundation for diagnostics, prognostics and targeted therapeutics. Systematic efforts to analyze cancer genomes are underway, but the analysis is hampered by the lack of a statistical framework to distinguish meaningful events from random background aberrations. Here, we describe a systematic method called Genomic Identification of Significant Targets in Cancer (GISTIC) designed for analyzing chromosomal aberrations in cancer. We use it to study chromosomal aberrations in 141 gliomas and compare the results with two prior studies. Traditional methods highlight hundreds of altered regions with little concordance between studies. The new approach reveals a highly concordant picture involving ~35 significant events, including 16-18 broad events near chromosome-arm size and 16-21 focal events. About half of these events correspond to known cancer-related genes, only some of which have been previously tied to glioma. We also show that superimposed broad and focal events may have different biological consequences. Specifically, gliomas with broad amplification of chromosome 7 have different properties than those with overlapping focal *EGFR* amplification: the broad events act in part through effects on *MET* and its ligand *HGF* and correlate with MET dependence *in vitro*. Our results support the feasibility and utility of systematic characterization of the cancer genome.

Introduction

Comprehensive knowledge of the mutational events responsible for cancer is a critical foundation for future diagnostics, prognostics and targeted therapeutics. Various efforts are now underway aimed at systematically obtaining this information. The first challenge in such a program is to study large collections of tumors to characterize the alterations that have occurred in their genomes. With recent advances in genomic technology, this is becoming increasingly feasible. For example, DNA arrays containing probes for hundreds of thousands of genetic loci have made it possible to detect regional amplifications and deletions with high resolution. Once the genomic alterations have been detected, the second challenge is to distinguish between 'driver' mutations that are functionally important changes (that is, that confer a biological property that allows the tumor to initiate, grow or persist) and 'passenger' mutations that represent random somatic events (that is, changes that occurred prior to a clonal expansion and are simply carried along despite conferring no selective advantage).

The importance of this second challenge is evident from recent studies of chromosomal aberrations in cancer. Strikingly, different studies of the same tumor type often report 'regions of interest' that are highly discordant. For example, two recent studies of lung cancer, with similar sample sizes and analytic methods, reported 48 and 93 regions of interest, respectively (1, 2); the overlap between the lists was less than 5%.

While perfect agreement should not be expected (in part due to differences in analytic methods), such high level of discordance is disconcerting. There are two potential explanations. One possibility is that the true number of cancer-related regions is extremely large, with each tumor containing only a small and variable subset of the alterations and each study detecting only a small subset of the regions. An alternative possibility is that many of the regions of interest reported in current studies are random events of no biologic significance, such as random passenger mutations. Current analysis methods do

not explicitly account for the background rate of random chromosomal aberrations. Similar issues arise in interpreting studies of point mutations in cancer resequencing projects (3-6).

In this paper, we describe a statistical approach, called Genomic Identification of Significant Targets in Cancer (GISTIC), for identifying regions of aberration that are more likely to drive cancer pathogenesis. The method identifies those regions of the genome that are aberrant more often than would be expected by chance, with greater weight given to high-amplitude events (high-level copy-number gains or homozygous deletions) that are less likely to represent random aberrations.

We then apply GISTIC to a newly generated, high-resolution dataset of chromosomal aberrations in 141 gliomas. Glioma is an excellent model in which to test the approach because the functional roles of a substantial number of copy number alterations have already been validated in preclinical models (7, 8). We find 32 statistically significant events of genomic amplification or loss. Using standard analytic methods, the regions of interest found in this study and those reported in two other recent studies of glioma are highly discordant. Strikingly, we find that the discordance largely vanishes when the GISTIC methodology is applied to the underlying data from all three studies. Moreover, the regions we find contain nearly all cancer genes previously known to be involved in glioma.

The significant aberrations in the glioma genome fall into two types: focal and broad (near the size of a chromosome arm). By studying the biological properties of tumors, we find evidence that overlapping focal and broad events can have very different consequences. Focusing on chromosome 7 (chr7), we show that focal high-level amplification at the *EGFR* gene is associated with activation of *EGFR* itself while broad lower-level amplification of the whole chromosome often activates the *MET* axis by increasing the dosage of both *MET* and its ligand *HGF*, suggesting that a subset of GBM patients with polysomy 7 might benefit from MET inhibition.

Results

GISTIC methodology

GISTIC identifies significant aberrations through two key steps (**Fig. 1**, **SI Methods**). First, the method calculates a statistic (*G* score) that involves both the frequency of occurrence and the amplitude of the aberration. Second, it assesses the statistical significance of each aberration by comparing the observed statistic to the results that would be expected by chance, using a permutation test that is based on the overall pattern of aberrations seen across the genome. The method accounts for multiple hypothesis testing using the false-discovery rate (FDR) framework (9) and assigns a q-value to each result, reflecting the probability that the event is due to chance fluctuation. For each significant region, the method defines a 'peak region' with the greatest frequency and amplitude of aberration. Each peak is tested to determine whether the signal is due primarily to broad events, focal events, or overlapping events of both types.

Application to glioma

We applied the method to a collection of 141 gliomas, including 107 primary glioblastomas (GBMs), 15 secondary GBMs, and 19 lower-grade gliomas (**SI Table 1**). We hybridized genomic DNA to microarrays containing probes for ~100,000 SNPs to identify copy-number changes and loss-of-heterozygosity (LOH). A genome-wide view of the copy-number alterations is shown in **Fig. 2a** (LOH results are described in **SI Note 1**). The overall pattern is complex, with almost every region of the genome being altered in at least one tumor. Nonetheless only 16 broad and 16 focal events are significant. Focal events are superimposed on four broad events (including two focal events on chromosome 7 and single events on chromosomes 9, 10, and 13), resulting in a total of 28 peak regions of amplification, deletion, and LOH.

The 16 broad events include 6 amplifications (chromosomes 7, 8q, 12p, 17q, 19p, and 20), 9 deletions (6q, 9p, 10, 11p, 13, 14, 16q, 19q, and 22), and 1 region of copy-neutral LOH (17p) (**Fig. 2b**, **SI Table 2**; **SI Note 1**). These events occur at high frequency (range 10-70%, median 27%). In particular, amplification of chr7 and deletion of chr10 each affect over 60% of our samples including over 80% of our primary GBMs. For broad regions without superimposed focal events, the peak regions are large (median of 110 genes) (**SI Table 2**).

The 16 focal events tend to occur at lower frequencies than the broad aberrations (range 6-49%, median 14%) (**SI Table 2**). Among these, amplifications of 4q12 and 7p11.2 (18-26% of samples) and deletions of 1p36.31 and 9p21.3 (35-49%) are the most frequent. In some cases, a high degree of amplification renders amplifications highly significant even though they occur in only 6-7% of samples (for example, the regions containing *CDK4* and *MDM2* on chr12). Because the background rate of deletions across the genome is higher, deletions usually must occur at higher frequencies than amplifications to attain similar levels of significance (**SI Table 2**). The peak regions for these focal events can be localized to small regions (median of 4 genes).

Analysis confirms known genes, identifies new loci

We compared the 28 peak regions to the locations of oncogenes and tumor-suppressor genes previously implicated in the pathogenesis of glioma. A recent review (10) lists 12 such genes reported to be altered in multiple studies of glioma (*TP53*, *RB1*, *CDKN2A/B*, *PTEN*, *EGFR*, *PDGFRA*, *MET*, *CDK4*, *CDK6*, *MDM2*, *MDM4*, *MYC*). We found that 11 of these 12 genes each correspond with one of the 28 peak regions (with one of these, *MYC*, laying just beyond the boundaries defined by GISTIC; as described below, this slight discrepancy is resolved with additional data) (**SI Table 2**). The twelfth gene (*CDK6*) lies within the broad region of significant amplification on chr7, although it does not correspond

to a peak. Interestingly, *TP53* is within the single peak region of LOH that is not reflected in a peak of copy-number change, suggesting that it is primarily inactivated through copy-neutral LOH (**SI Note 1**).

An additional 5 peak regions contain genes that are known to play a role in other cancers (*MYCN*, *PIK3CA*, *CCND2*, *KRAS*, and *CHD5*) (11, 12). Our analysis suggests that chromosomal aberrations involving these genes are also relevant for glioma pathogenesis. These genes should therefore be carefully characterized in glioma.

The remaining 12 regions (43% of the total) are not associated with known cancer-related genes. These events occur at substantial frequencies (6-37%), but nine are due to broad events and two others rarely reach high amplitude. The final region (12q14.3) undergoes high-level amplifications, but always in concert with amplifications of either of two neighboring regions containing *CDK4* and *MDM2* (data not shown), suggesting it may be due to structural features required to amplify these genes (as is the case in dedifferentiated liposarcoma (13, 14)). The fact that nearly half the regions (including regions affected by highly prevalent aberrations) are not yet associated with known cancer-related genes underscores the importance of systematic analysis of the cancer genome.

Previous studies of copy-number alterations in glioma have shown distinct patterns for certain subtypes such as primary vs secondary GBMs (15) or astrocytic vs oligodendroglial tumors (16). To explore whether our combined analysis of these glioma subtypes prevented the detection of alterations specific to primary GBMs, we performed a separate analysis on only the 107 primary GBMs in out sample set. No additional statistically significant alterations were identified (**SI Fig. 1**)

Consistency across independent datasets

We then sought to compare our results with two previous studies of copy-number alterations in glioma (178 samples on 100K SNP arrays; 37 samples on a 16K CGH array) (15, 17). At first glance, there appear to be striking differences. The previous studies reported many more regions of interest (208

and 97) (**Table 1**), but the regions included fewer of the known glioma-associated genes and show low concordance with one another. The differences are attributable to the methodology used in these studies, in which minimal common regions of copy-number change are reported, without explicitly taking into account the degree of background noise (see **SI Note 2**). Applying a similar analysis to our own data identifies a similarly large number of regions (144) (see **SI Note 2**) but these include fewer known glioma-associated genes and show low concordance with the other studies. By contrast, applying GISTIC to the raw data from the other two studies identifies 24 and 26 significant regions each. Importantly, these regions agree closely with the 27 regions (excluding copy-neutral LOH of 17p, as it is not observed in the copy-number analyses) identified above (**SI Fig. 2**), and they include essentially the same glioma-associated genes. Moreover, these results are specific to glioma, as seen in a comparison to lung cancer (**SI Fig. 3**) (2). The strong concordance across three independent datasets and two different platforms supports the validity of both the GISTIC methodology and our results for glioma.

Given the close agreement across these datasets, we combined our initial dataset with the data from the prior study performed on the same platform to obtain a pooled dataset with 319 glioma samples. This analysis identified 34 significant regions, including 27 of the 28 identified in the initial dataset (**SI Table 2**). For the additional regions, the prevalence of aberrations is similar in the initial and combined datasets (11.0% vs. 11.3%), but they now exceed the significance threshold due to the larger sample size. Increasing the sample size also leads to narrower regions, with the median number of genes decreasing from 12 to 5 per region. Inclusion of additional datasets may define these regions with even greater precision and facilitate identification of the gene targets.

Overlapping broad and focal events may have different consequences

Having identified various instances of overlapping broad and focal events, we explored whether they have distinct functional consequences, using chr7 as an example (**SI Fig. 4**). We first compared

copy-number profiles to gene expression among a group of 43 primary GBMs for which we had sufficient material for a combined analysis. *EGFR* was overexpressed in most GBMs with focal *EGFR* amplification ('7^{gain}EGFR^{amp}') but in none of the GBMs with broad amplification of chromosome 7 in the absence of focal *EGFR* amplification ('7^{gain}') (**Fig. 3a**). We found three additional sources of evidence supporting the biologic distinction between these two classes of tumors. First, recognizing that *EGFR*-amplified tumors are known to carry a low rate of mutations in the *TP53* gene (18), we sequenced *TP53* and found these mutations more frequently associated with 7^{gain} compared to 7^{gain}EGFR^{amp} (two-sided Fisher's exact p = 0.03). Second, we found that 7^{gain} is less frequently associated with *EGFR* point mutations or expression of the EGFRvIII deletion mutant (determined for many of our tumors in a prior study (19)) (p = 0.001). Third, we found that 7^{gain} but not 7^{gain}EGFR^{amp} occurs frequently in secondary GBMs (p = 0.16). These three findings are consistent with earlier observations regarding 7^{gain}EGFR^{amp} (20, 21), and further suggest that 7^{gain} has distinct functional consequences.

To explore the function of 7^{gain}, we identified genes on the chromosome that show extreme outliers in expression in at least 10% of tumors with 7^{gain}, compared to 7^{normal} (**SI Note 3**). The notion behind this 'comparative outlier analysis' is that broad events such as 7^{gain} may have heterogeneous effects across various tumors. We are interested in identifying genes that are strongly upregulated in even a subset of the samples.

Strikingly, two of the top four genes in this analysis are those encoding the receptor MET and its ligand HGF (**SI Table 3**). Approximately one-third of 7^{gain} events are associated with either *MET* or *HGF* overexpression (**Fig. 3a**), and tumors that overexpress one tend to overexpress both (p = 0.06) (data not shown). The overexpression of *MET* and *HGF* appears to be functionally relevant: we studied glioma cell lines with 7^{gain} and increased expression of *MET* and *HGF* (**Fig. 3b**) and found

phosphorylation and activation of the MET receptor even under serum-starved conditions (**Fig. 3c**). These cell lines showed enhanced responsiveness to the MET kinase inhibitor SU11274 (22) (**Fig. 3d**) at drug concentrations that inhibit the MET signaling pathway (**SI Fig. 5a-b**). None of the GBM cell lines with 7^{gain} showed constitutive activation of EGFR or were responsive to the EGFR kinase inhibitor erlotinib (**SI Fig. 5c-d**). Compared to the relatively rare (5-7%) focal amplification of the *MET* gene locus (**SI Table 2**), 7^{gain} with overexpression of *MET* and *HGF* may provide a more common mechanism for cell autonomous activation of the MET signaling pathway in glioma. This finding may be relevant for the clinical deployment of inhibitors targeting this network in glioma and other cancers (23).

Discussion

The application of a statistical approach such as GISTIC to the panoply of chromosomal aberrations found in cancer identifies those recurrent changes that are concordant across datasets and less likely to represent random passenger events. Indeed, we have now successfully used this approach to identify biologically significant aberrations in lymphoma (24), melanoma (25), and lung cancer (26). Although it is likely that the majority of the events identified by GISTIC are drivers that recur due to the effects of positive selection during tumor evolution, some events may recur due to biases in the DNA repair machinery for which our model of background aberrations does not account. Likewise, some driver aberrations may occur at low frequency and therefore be missed. The design of future experiments should consider the number of tumors needed to power detection of such rare events.

Ultimately, the utility of systematic efforts to characterize the cancer genome is an empirical question. There are at least two potential concerns: on one hand, that the vast majority of cancer-related genes are already known with little left to learn; on the other hand, that cancer is hopelessly complicated,

with a large number of cancer genes, each altered in a small fraction of tumors. The results here suggest a more favorable situation, at least for copy-number alterations. With appropriate statistical methodology, three studies reveal a concordant picture of the glioma genome. There appears to be a tractable number of recurrent events, in the range of 40. Larger tumor collections may identify some additional low-prevalence events, but it seems likely that the majority of significant recurrent copy-number alterations at this scale have been found. About half are likely to involve known cancer-related genes, with some not having previously been established to be involved in glioma; all of these genes should be systematically characterized in glioma. The remaining events likely point to cancer-related genes and other functional elements that remain to be discovered; the identification of the genes associated with the broad events is particularly important and will likely require the application of orthogonal approaches, such as expression profiling, mutational analysis and RNA interference. Finally, copy-number aberrations are only one form of the genomic changes in glioma. Identification of other cancer-associated events, including mutations, rearrangements, and epigenetic alterations will require similar statistical approaches and large data sets, as presented here.

Methods

Clinical samples and cell lines

Genomic DNA was extracted from fresh frozen tumors samples using DNeasy (Qiagen). Non-tumor tissue, including paired normal brain corresponding to ten gliomas, was used for germline control DNA. Collection and analysis of all clinical samples was approved by the UCLA Institutional Review Board. RNA and DNA were also obtained from the GBM cell lines 8-MG-BA, A172, DK-MG, GAMG, HS683, LN-18, SF-268, SF-295, SNB-75, T98G, and U251. Gastric and lung cancer cell lines MKN-45 (high level *MET* amplified) and H3255 (L858R *EGFR* mutant) were included as positive controls in experiments with the *MET* kinase inhibitor SU11274 and the *EGFR* kinase inhibitor erlotinib, respectively.

SNP Arrays

Genomic DNA was applied according to manufacturer's instructions to oligonucleotide arrays (Affymetrix) interrogating 116,204 SNP loci on all chromosomes except Y (www.affymetrix.com). Arrays were scanned using the GeneChip Scanner 3000 and genotyping was performed using Affymetrix Genotyping Tools Version 2.0. Probe-level signal intensities were normalized to a baseline array with median intensity using invariant set normalization (27). SNP-level signal intensities were obtained using a model-based (PM/MM) method (28). Further analytic steps are described in **SI Methods**. SNP, gene, and cytogenetic band locations are based on the hg16 (July 2003) genome build (http://genome.ucsc.edu). Data from SF-268, SF-295, SNB-75, and six gliomas (along with paired normals) were previously published (29, 30).

Mutation detection

PTEN and *TP53* were sequenced in 134 of the 141 samples undergoing SNP analysis as previously described (19). All exons were covered in over 70% of samples except exons 1, 8, and 9 in *PTEN* and exons 7 and 10 in *TP53*. *EGFR* point mutations and vIII expression were determined for 133 and 58 samples respectively in a prior study (19).

Expression arrays

Expression data were obtained using Affymetrix U133A/B and plus 2 arrays from 43 primary GBMs undergoing SNP array analysis. CEL files from U133A and plus 2 arrays were preprocessed separately using RMA (31). Probesets common to both arrays were used after equalizing the mean and standard deviation of the U133A and plus 2 arrays. Expression data from GBM cell lines were generated by Affymetrix cartridge arrays, except SF-268, SF-295, and SNB-75, where available U133A data were used (http://wombat.gnf.org/index.html).

***EGFR* and *MET* inhibition**

Cell proliferation assays

Cell lines were maintained in RPMI containing 10% serum and 1% penicillin/streptomycin. Stock solutions of of erlotinib (10 mM; WuXi Pharmatech) and SU11274 (1mM; Calbiochem) were prepared in DMSO and maintained at -20C or 4C according to manufacturer's instructions. Drugs were diluted in fresh medium prior to each experiment. Cells were cultured in the presence of drug or vehicle for 4 days and viability was determined using the WST assay (Roche) or trypan blue exclusion assay as previously described (32, 33).

Western blot analysis

To examine basal MET and EGFR phosphorylation, cells were grown in serum-free DMEM with 1% L-glutamine 200mM, and 1% Pen/Strep for 24 hours. Cells were harvested and lysed using cell lysis buffer (Cell Signaling Technology) with 1% protease and 1% phosphatase inhibitors (Calbiochem). Total protein concentration was determined using Bio-Rad Protein Assay Standard I (Bio-Rad Laboratories). Equal protein amounts were resolved by SDS-PAGE and electro-transferred to nitrocellulose membrane blots (34). Blots were probed with antibodies against MET (25H2), P-MET (P-Tyr 1234/5), P-EGFR (P-Tyr 1173) (Cell Signaling Technology), and EGFR (sc-03; Santa Cruz Biotechnology), and exposed to standard X-ray film after application of peroxidase-conjugated secondary antibodies (Jackson-Immuno Research Lab) and ECL western blotting detection reagents (GE Healthcare).

Acknowledgements

This work was supported by funds from the Broad Institute of Harvard and MIT, the Dana-Farber/Harvard Cancer Center Prostate SPORE (R.B.), DOD grant PC040638 (R.B.), NCI grants CA109038 and CA126546 (M.M,), the Henry E. Singleton Brain Cancer Program at UCLA, Accelerate Brain Cancer Cure (I.K.M.), and the Brain Tumor Funders' Collaborative. J.B. is a Beatriu de Pinos Fellow of the Departament d'Educació i Universitats de la Generalitat de Catalunya. J.D. and R.K.T.are supported by fellowships of the Leukemia and Lymphoma Society and International Association for the Study of Lung Cancer and R.K.T. is a Mildred-Scheel fellow of the Deutsche Krebshilfe. I.K.M. is a Sontag Foundation Distinguished Scientist. Nadav Kupiec and Bang Wong provided help with illustrations. Howard Fine, Elizabeth Maher, Cameron Brennan, Ron Depinho, and Lynda Chin provided data.

Figure Legends

Figure 1. Overview of the GISTIC method. After identifying the locations and, in the case of copy-number alterations, magnitudes (as $\log_2$ signal intensity ratios) of chromosomal aberrations in multiple tumors (left panel), GISTIC scores each genomic marker with a *G* score that is proportional to the total magnitude of aberrations at each location (middle panel, top). In addition, by permuting the locations in each tumor, GISTIC determines the frequency with which a given score would be attained if the events were due to chance and therefore randomly distributed (middle panel, bottom). A significance threshold (green line) is determined such that significant scores are unlikely to occur by chance alone. Alterations are deemed significant if they occur in regions that surpass this threshold (right panel). For more details, see SI Methods.

Figure 2. Significant broad and focal copy-number alterations in the glioma genome. (a) Amplifications (red) and deletions (blue), determined by segmentation analysis of normalized signal intensities from 100K SNP arrays (see SI Methods), are displayed across the genome (chromosome positions, indicated along the y axis, are proportional to marker density) for 141 gliomas (x axis; diagnosis is displayed on top and gliomas with low purity are segregated to the right). Broad events near the size of a chromosome arm are the most prominent, including amplifications of chr7 and deletions of chr10 observed among more than 80% of GBMs. (b) GISTIC analysis of copy-number changes in glioma. The statistical significance of the aberrations identified in (a) are displayed as FDR q-values (9) to account for multiple hypothesis testing. Chromosome positions are indicated along the y axis with centromere positions indicated by dotted lines. Fifteen broad events (indicated by red bars for amplifications and blue bars for deletions) and sixteen focal events (indicated by dashes) surpass the significance threshold (green line). The locations of the peak regions and the known cancer-related

genes within those peaks are indicated to the right of each panel. Several broad regions, including chr7 and chr10, contain superimposed focal events, leading to needle-shaped peaks superimposed on highly significant plateaus.

Figure 3. Broad gains of chromosome 7 often activate the MET pathway but not EGFR. (a) Expression levels of *EGFR*, *MET*, and its ligand *HGF* (all located on chr7) in primary GBMs. These data are $\log_2$-transformed signal intensities from all concordant probesets for each gene from Affymetrix U133 arrays, centered and normalized according to the median and median absolute deviation of samples with 7^{norm}. Samples with $7^{gain}EGFR^{amp}$ but not 7^{gain} overexpress *EGFR* (highlighted in red) relative to 7^{norm}. Conversely, a subset of tumors with 7^{gain} overexpress *MET* or its ligand *HGF*, even in the absence of focal amplification. (b) A subset of glioma cell lines with 7^{gain} also overexpress *MET* and *HGF* (MET/HGF^+ lines, highlighted in red). We characterized lines as having 7^{gain} if SNP array analysis showed them to be amplified across most of chr7. Cell lines are classified as being *MET* dependent based either on the results shown in panel (d) or previously published results (asterisks) (35). (c) Consitutive phosphorylation of MET in MET/HGF^+ lines. Immunoblots to the indicated epitopes were performed on whole-cell lysates prepared after 24-hour serum starvation. Decreased MET protein levels in activated lines are a result of HGF-induced degradation (36). *MET*-dependent gastric cancer cells (MKN-45) were included as positive controls (35). (d) Decreased viability of MET/HGF^+ cell lines (red) compared to non- MET/HGF^+ lines (black) when treated with the MET inhibitor SU11274. Viability was measured using Trypan blue exclusion after exposure to inhibitor at the indicated concentrations for 96 hours. MKN-45 cells (blue) were included as positive controls.

References:

1. Tonon G, Wong KK, Maulik G, Brennan C, Feng B, Zhang Y, Khatry D, Protopopov A, You MJ, Aguirre AJ, et al (2005) *Proc Natl Acad Sci U S A* **102,** 9625-9630.
2. Zhao X, Weir BA, LaFramboise T, Lin M, Beroukhim R, Garraway L, Beheshti J, Lee JC, Naoki K, Richards WG, et al (2005) *Cancer Res* **65,** 5561-5570.
3. Davies H, Hunter C, Smith R, Stephens P, Greenman C, Bignell G, Teague J, Butler A, Edkins S, Stevens C, et al (2005) *Cancer Res* **65,** 7591-7595.
4. Greenman C, Stephens P, Smith R, Dalgliesh G, Hunter C, Bignell G, Davies H, Teague J, Butler A, Stevens C, et al (2007) *Nature* **446,** 153-8.
5. Sjoblom T, Jones S, Wood LD, Parsons DW, Lin J, Barber TD, Mandelker D, Leary RJ, Ptak J, Silliman N, et al (2006) *Science* **314,** 268-74.
6. Getz G, Höfling H, Mesirov JP, Golub TR, Meyerson ML, Tibshirani R & Lander ES (2007) *Science* **317,** 1500.
7. Maher EA, Furnari FB, Bachoo RM, Rowitch DH, Louis DN, Cavenee WK & DePinho RA (2001) *Genes Dev* **15,** 1311-33.
8. Fomchenko EI & Holland EC (2006) *Clin Cancer Res* **12,** 5288-97.
9. Benjamini Y & Hochberg Y (1995) *J Roy Stat Soc, Ser B* **57,** 289-300.
10. Reifenberger G & Collins VP (2004) *J Mol Med* **82,** 656-70.
11. Futreal PA, Coin L, Marshall M, Down T, Hubbard T, Wooster R, Rahman N & Stratton MR (2004) *Nat Rev Cancer* **4,** 177-83.
12. Bagchi A, Papazoglu C, Wu Y, Capurso D, Brodt M, Francis D, Bredel M, Vogel H & Mills AA. (2007) *Cell* **128,** 459-75.
13. Mandahl N, Heim S, Johansson B, Bennet K, Mertens F, Olsson G, Rooser B, Rydholm A, Willen H & Mitelman F (1987) *Int J Cancer* **39,** 685-8.
14. Pedeutour F, Forus A, Coindre JM, Berner JM, Nicolo G, Michiels JF, Terrier P, Ranchere-Vince D, Collin F, Myklebost O & Turc-Carel C (1999) *Genes Chromosomes Cancer* **24,** 30-41.
15. Maher EA, Brennan C, Wen PY, Durso L, Ligon KL, Richardson A, Khatry D, Feng B, Sinha R, Louis DN, et al (2006) *Cancer Res* **66,** 11502-13.
16. Kraus JA, Koopmann J, Kaskel P, Maintz D, Brandner S, Schramm J, Louis DN, Wiestler OD & von Deimling A (1995) *J Neuropathol Exp Neurol* **54,** 91-5.
17. Kotliarov Y, Steed ME, Christopher N, Walling J, Su Q, Center A, Heiss J, Rosenblum M, Mikkelsen T, Zenklusen JC & Fine HA (2006) *Cancer Res* **66,** 9428-36.
18. Watanabe K, Tachibana O, Sata K, Yonekawa Y, Kleihues P & Ohgaki H (1996) *Brain Pathol* **6,** 217-23; discussion 23-4.
19. Lee JC, Vivanco I, Beroukhim R, Huang JH, Feng WL, Debiasi RM, Yoshimoto K, King JC, Nghiemphu P, Yuza Y, et al (2006) *PLoS Med* **3,** e485.
20. Galanis E, Buckner J, Kimmel D, Jenkins R, Alderete B, O'Fallon J, Wang CH, Scheithauer BW & James CD (1998) *Int J Oncol* **13,** 717-24.
21. Ekstrand AJ, Sugawa N, James CD & Collins VP (1992) *Proc Natl Acad Sci U S A* **89,** 4309-13.
22. Sattler M, Pride YB, Ma P, Gramlich JL, Chu SC, Quinnan LA, Shirazian S, Liang C, Podar K, Christensen JG & Salgia R (2003) *Cancer Res* **63,** 5462-9.
23. Birchmeier C, Birchmeier W, Gherardi E & Vande Woude GF (2003) *Nat Rev Mol Cell Biol* **4,** 915-25.
24. Takeyama K, Monti S, Manis JP, Cin PD, Getz G, Beroukhim R, Dutt S, Aster JC, Alt FW, Golub TR & Shipp MA (2007) *Oncogene*.

25. Lin WM, Baker AC, Beroukhim R, Winckler W, Feng W, Marmion J, Laine E, Greulich H, Tseng H, Gates C, et al (in press) *Cancer Res*.
26. Weir BA, Woo MS, Getz G, Perner S, Ding L, Beroukhim R, Lin WM, Province MA, Kraja A, Johnson LA, et al (in press) *Nature*.
27. Li C & Wong WH (2001) *PNAS* **98,** 31-36.
28. Li C & Wong WH (2001) *Genome Biology* **2,** research0032.1 - research0032.11.
29. Beroukhim R, Lin M, Park Y, Hao K, Zhao X, Garraway LA, Fox EA, Hochberg EP, Mellinghoff IK, Hofer MD, et al (2006) *PLoS Comput Biol* **2,** e41.
30. Garraway LA, Widlund HR, Rubin MA, Getz G, Berger AJ, Ramaswamy S, Beroukhim R, Milner DA, Granter SR, Du J, et al (2005) *Nature* **436,** 117.
31. Irizarry RA, Hobbs B, Collin F, Beazer-Barclay YD, Antonellis KJ, Scherf U & Speed TP (2003) *Biostatistics* **4,** 249-64.
32. Greulich H, Chen TH, Feng W, Janne PA, Alvarez JV, Zappaterra M, Bulmer SE, Frank DA, Hahn WC, Sellers WR & Meyerson M (2005) *PLoS Med* **2,** e313.
33. Mellinghoff IK, Wang MY, Vivanco I, Haas-Kogan DA, Zhu S, Dia EQ, Lu KV, Yoshimoto K, Huang JH, Chute DJ, et al (2005) *N Engl J Med* **353,** 2012-24.
34. Mellinghoff IK, Tran C & Sawyers CL (2002) *Cancer Res* **62,** 5254-9.
35. Smolen GA, Sordella R, Muir B, Mohapatra G, Barmettler A, Archibald H, Kim WJ, Okimoto RA, Bell DW, Sgroi DC, et al (2006) *Proc Natl Acad Sci U S A* **103,** 2316-21.
36. Jeffers M, Taylor GA, Weidner KM, Omura S & Vande Woude GF (1997) *Mol Cell Biol* **17,** 799-808.

Figure 1

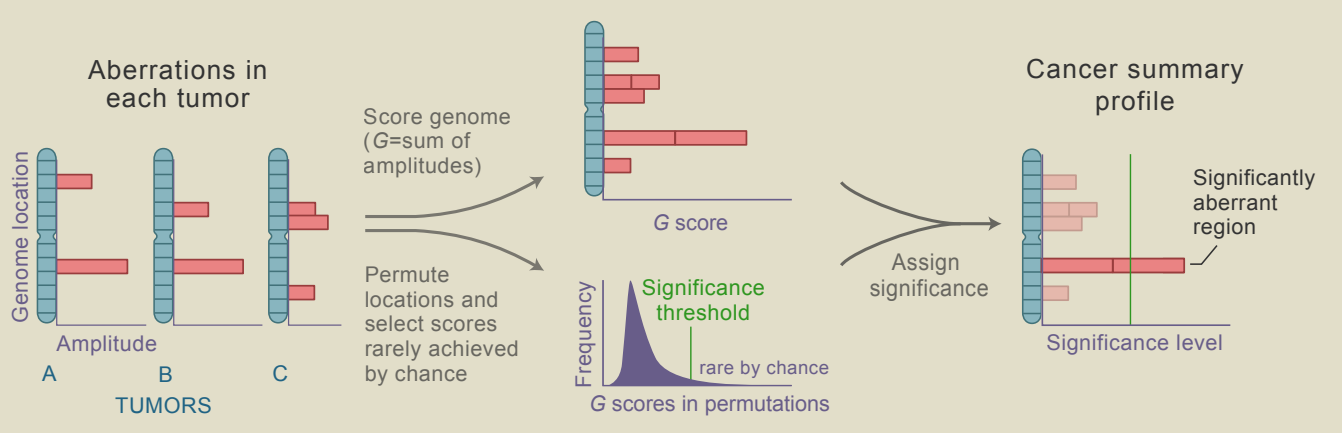
Aberrations in each tumor
Genome location
Amplitude
A
B
C
TUMORS
Score genome (G=sum of amplitudes)
Permute locations and select scores rarely achieved by chance
G score
Frequency
Significance threshold
rare by chance
G scores in permutations
Assign significance
Cancer summary profile
Significantly aberrant region
Significance level

Figure 2

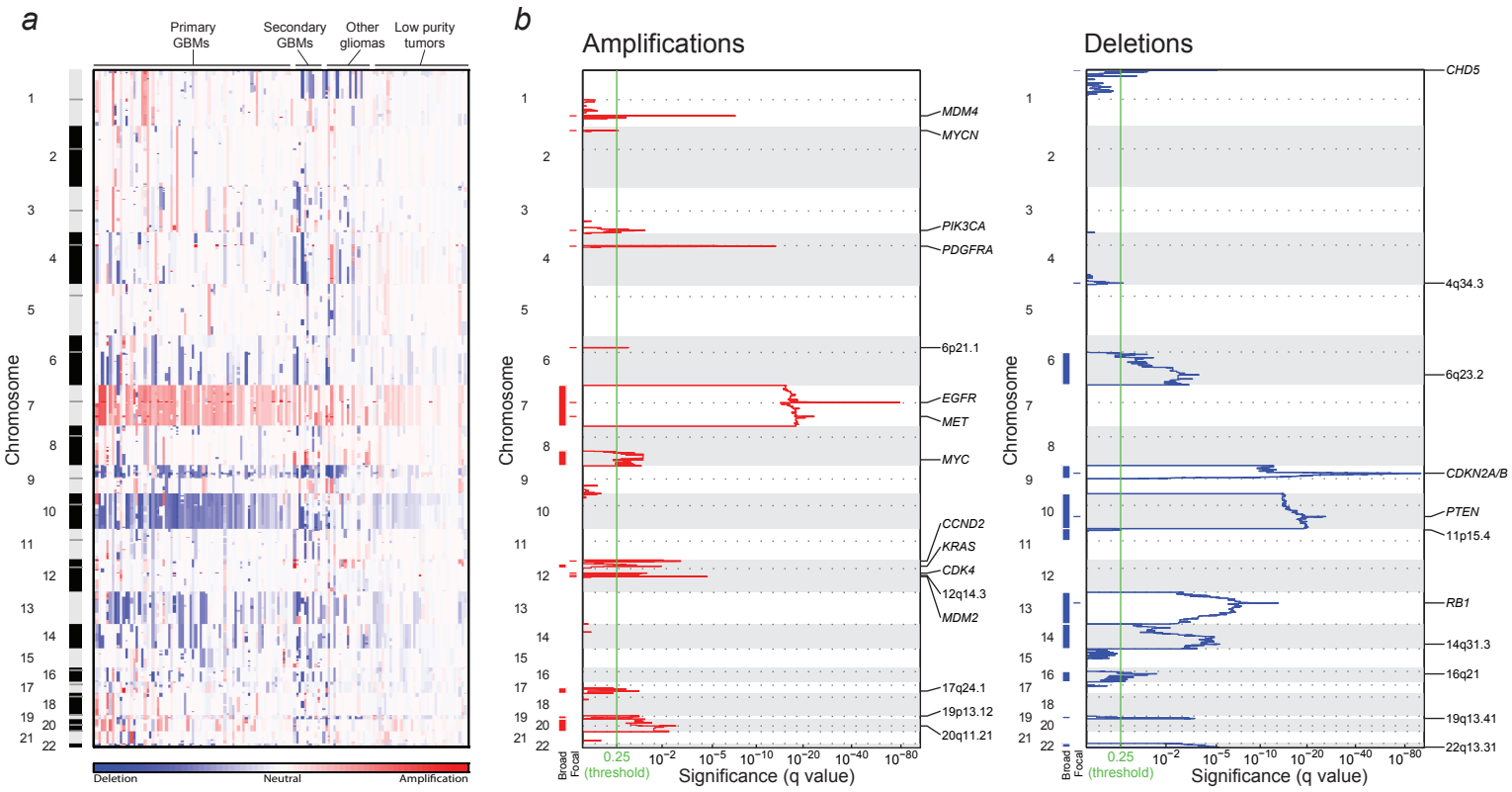
a
Primary GBMs
Secondary GBMs
Other gliomas
Low purity tumors
Chromosome
Deletion
Neutral
Amplification
b
Amplifications
Deletions
MDM4
MYCN
PIK3CA
PDGFRA
6p21.1
EGFR
MET
MYC
CCND2
KRAS
CDK4
12q14.3
MDM2
17q24.1
19p13.12
20q11.21
CHD5
4q34.3
6q23.2
CDKN2A/B
PTEN
11p15.4
RB1
14q31.3
16q21
19q13.41
22q13.31
Broad
Focal
0.25
(threshold)
Significance (q value)

Figure 3

a

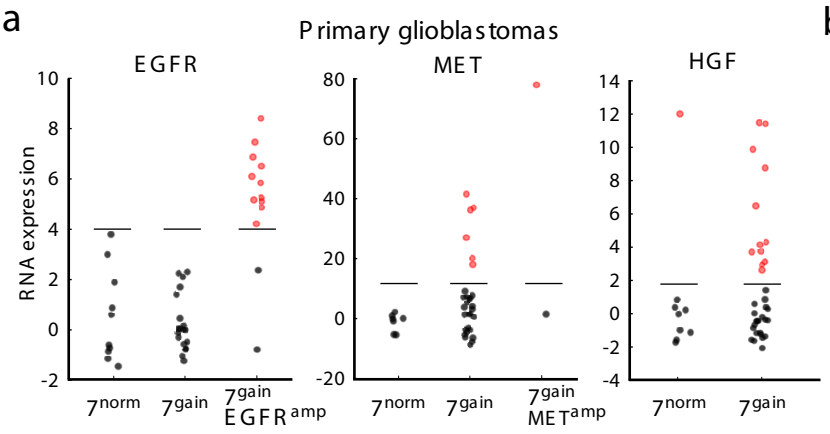

b

Cell line	Chr7	RNA expression MET	HGF	MET dependent?
8-MG-BA		-1.19	-0.47	No
M059K		-0.32	1.44	No*
A172	gain	-1.22	-0.61	No*
SF268	gain	-0.16	-0.09	No
SNB75	gain	-0.52	-0.90	No
T98G	gain	-1.16	-1.13	No*
U251	gain	-0.85	-0.68	No
GA-MG	gain	1.21	-0.19	No
DK-MG	gain	1.04	1.62	Yes
HS683	gain	1.05	1.19	Yes
LN18	gain	0.75	0.98	Yes
SF295	gain	0.95	1.60	Yes

c

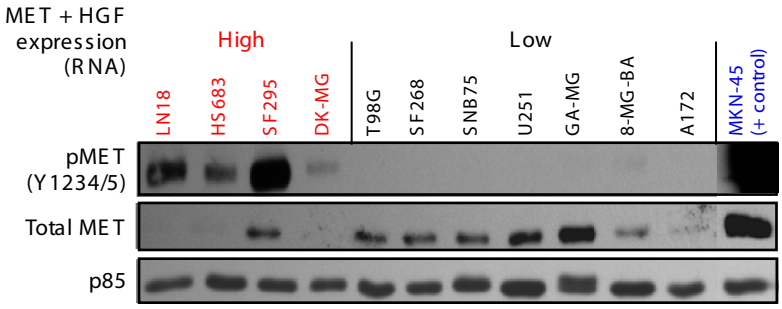

d

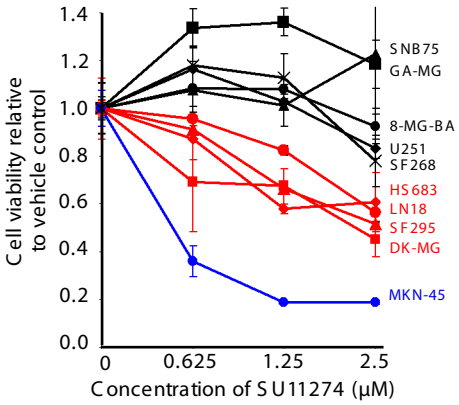

Table 1 Comparison of results between copy-number analyses of the glioma genome

			MCR analysis†		GISTIC analysis	
Dataset	Platform	# of tumors	# of MCRs	# of glioma genes in MCRs*	# of peaks	# of glioma genes in peaks*
Initial	100K SNP	141	144	5	27	9
Kotliarov (17)	100K SNP	178	208	3	26	9
Maher (15)	16K aCGH	37	97	8	24	9

* Eleven glioma genes affected by copy-number aberrations are considered "known": PTEN, RB1, CDKN2A/B, EGFR, PDGFRA, MET, CDK4, CDK6, MDM2, MDM4, and MYC (10)

† Minimal common regions (MCR) analysis, as presented in cited publications.